Structure refinements of superconducting $Tl_2Ba_2CaCu_2O_8$ and $Tl_2Ba_2Ca_2Cu_3O_{10}$ from neutron diffraction data

D. E. Cox
Physics Department, Brookhaven National Laboratory, Upton, New York 11973

C. C. Torardi, M. A. Subramanian, J. Gopalakrishnan, and A. W. Sleight
Central Research and Development Department, E. I. du Pont de Nemours and Company, Experimental Station, Wilmington, Delaware 19898
(Received 28 April 1988)

The structures of $Tl_2Ba_2CaCu_2O_8$ and $Tl_2Ba_2Ca_2Cu_3O_{10}$ were refined from neutron-powder-diffraction data. The data for $Tl_2Ba_2CaCu_2O_8$ were taken at 298 K, and the data for $Tl_2Ba_2Ca_2Cu_3O_{10}$ were obtained at both 150 and 13 K. The results are essentially in agreement with the structural refinements based on single-crystal x-ray-diffraction data and confirm the positional disorder of the oxygen atoms in the Tl-O planes. The low-temperature refinements for $Tl_2Ba_2Ca_2Cu_3O_{10}$ indicate that the symmetry remains tetragonal down to 13 K and that there is no significant structural change or discontinuity in the cell parameters through the superconducting critical temperature near 125 K.

INTRODUCTION

Sheng, Hermann, and co-workers[1-3] have recently reported high-temperature superconductivity above 100 K in the Tl-Ba-Ca-Cu-O system. From electron and x-ray-diffraction measurements, Hazen *et al.*[4] identified tetragonal phases $Tl_2Ba_2CaCu_2O_{8+\delta}$ ($a=5.44$, $c=29.55$ Å) and $Tl_2Ba_2Ca_2Cu_3O_{10+\delta}$ ($a=5.40$, $c=36.25$ Å) and concluded the structures were closely related to that of $Bi_2Sr_2CaCu_2O_8$.[5-7] It is now known[8] that the superconducting phases in this system can be represented as $Tl_2Ba_2Ca_{n-1}Cu_nO_{2n+4}$ where n is the number of consecutive Cu-O layers. Values of n range from 1 to 3 in bulk phases but can range up to at least 5 on a microscopic level.[8] The superconducting transition temperature, T_c, is about 125 K for the $n=3$ phase and appears to be about 140 K for the $n=5$ phase.

From x-ray single-crystal data, the structures of the phases with $n=1$, 2, and 3 have been solved and refined.[8-10] The unit cells are tetragonal, space group $I4/mmm$, with $a\sim3.85$ Å and $c\sim23.2$, 29.3, and 35.9 Å, respectively. No evidence was found for any superlattice peaks indicative of an enlarged cell ($a=5.44$ Å) in either the single-crystal data or in x-ray powder diffraction measurements on bulk samples.

The structures are comprised of single,[9] double,[10] or triple[8] CuO_2 sheets, with Cu in square planar coordination, that alternately stack with sheets of barium ions, and double sheets of Tl-O atoms. When Ca is present, it is found between the Cu-O sheets. There is considerable disorder of the oxygens in the Tl-O sheets in the form of displacements of about 0.4 Å from the ideal positions.

The present paper describes the results of neutron-diffraction studies on polycrystalline samples, which, in view of the much greater sensitivity of neutrons to oxygen, provide useful complementary information about the structure. Structural refinements have been carried out for $Tl_2Ba_2CaCu_2O_8$ at 293 K, and for $Tl_2Ba_2Ca_2Cu_3O_{10}$ above (150 K) and below (13 K) the superconducting transition temperature.

EXPERIMENTAL DETAILS

Neutron-powder-diffraction measurements were made on a triple-axis diffractometer at the Brookhaven high-flux beam reactor equipped with a pyrolytic graphite monochromator and analyzer in the (002) and (004) settings, respectively. The collimation was 20′ in-pile, 40′ monochromator-sample, 40′ sample-analyzer, and 20′ analyzer-detector. The wavelength was 2.369 ± 0.001 Å, and the higher-order harmonics were eliminated with a pyrolytic graphite filter.

The synthesis procedures have been previously reported.[8] Flux exclusion measurements showed superconducting transition onset temperatures of 98 and 105 K, respectively, for the $Tl_2Ba_2CaCu_2O_8$ and $Tl_2Ba_2Ca_2Cu_3O_{10}$ samples. About 20 g of each material in the form of pressed pellets were placed in an aluminum sample holder. The holder containing $Tl_2Ba_2Ca_2Cu_3O_{10}$ was loaded into

TABLE I. Intensities and d spacings of impurity peaks in diffraction patterns from $Tl_2Ba_2CaCu_2O_8$ and $Tl_2Ba_2Ca_2Cu_3O_{10}$. Intensities are scaled with respect to a value of 100 for the strongest peak in the pattern in each case.

$Tl_2Ba_2CaCu_2O_8$		$Tl_2Ba_2Ca_2Cu_3O_{10}$	
d (Å)	I	d (Å)	I
4.53	4.0	4.52	2.7
3.04	4.9	2.38	3.8
2.54	3.5	2.26	1.5
2.42	3.7	1.66	1.8
2.25	1.9		
2.15	2.1		
1.76	4.3		

a closed-cycle He cryostat for temperature-dependence measurements. Extended data sets for Rietveld refinement were collected at 293 K for $Tl_2Ba_2CaCu_2O_8$ and at 150 and 13 K for $Tl_2Ba_2Ca_2Cu_3O_{10}$ by step scanning at 0.1° intervals over the angular range 5°–139°. In addition, shorter scans were performed over selected regions to monitor the behavior of the lattice parameters through the superconducting transition region.

A few weak peaks were observed in the diffraction patterns of both compounds that could not be indexed in terms of an enlarged $(a\sqrt{2},c)$ cell and were presumed to arise from small amounts of impurity phases. The d spacings and relative intensities of these are listed in Table I.

$Tl_2Ba_2CaCu_2O_8$

Rietveld refinement was carried out with a modified version of the Rietveld-Hewat program.[11,12] Impurity peaks and peaks from the Al sample holder were excluded, and background values were obtained by linear interpolation between average values in regions between peaks. The low-angle (002) reflection was not included because of severe asymmetry effects due to vertical divergence. Initially, Gaussian peak shapes were assumed, and intensities were calculated over an angular range of four full widths at half maximum. Subsequently, a slight improvement was obtained with a Lorentzian component to the peak width of the type $X\tan\theta$, where X is a refineable parameter. The total number of peaks in the refinement was 55, and the starting model involved 21 parameters, comprising 7 profile variables (half-width and unit-cell parameters and a zero-point correction) and 14 structural parameters (atomic positions, isotropic temperature factors and a scale factor). The atom positions were assigned the recently reported x-ray values[10] in space group $I4/mmm$ with the exception that O(3), the oxygen atom in the Tl sheets, was placed in the ideal position $(\frac{1}{2},\frac{1}{2},z)$. The refinement converged rapidly to positions close to the x-ray values but with a large B of 4.9 Å^2 for O(3), indicative of significant static displacements, and B values of -0.8 Å^2 and 1.1 Å^2 for Ca and Tl, respectively, which could arise from a slight amount of substitutional disorder. Further refinements were carried out to test these possibilities, and a preferred orientation parameter G of the type proposed by Rietveld[11] was also introduced in the later stages. A marked improvement in the fit was obtained when anisotropic temperature factors were assigned to O(3) [$B_{11}=7.8(3)$, $B_{33}=0.6(3)$ Å^2], or when this atom was statistically distributed in 16(n) sites, $(x,\frac{1}{2},z)$ surrounding the ideal $(\frac{1}{2},\frac{1}{2},z)$ site [$x=0.603(2)$, $B=0.5(3)$ Å^2]. A marginally poorer fit compared to the latter was obtained when O(3) was placed in the 16(m) sites at (x,x,z) [$x=0.570(2)$, $B=0.9(3)$ Å^2].

The results for the 16(n)-site model are listed in Table II, together with the commonly used residuals R_I (integrated intensities), R_{WP} (weighted profile), R_e (expected), and S_P^2 (profile goodness of fit). Also listed is S_I^2, which is based on integrated intensities and is probably a more realistic goodness-of-fit indicator.[13] If this were used instead of S_P^2 in the analysis, the estimated standard deviations (ESD's) would be about 2.5 times greater than those given in the table. The profile fit and difference plot are shown in Fig. 1.

Refinement of the O(3) site occupancy yielded the ideal

TABLE II. Results of Rietveld refinement for $Tl_2Ba_2CaCu_2O_8$ at 293 K. Scattering amplitudes for Tl, Ba, Ca, Cu, and O taken as 0.879, 0.525, 0.490, 0.7718, and 0.5805×10^{-12} cm, respectively (Ref. 16). Numbers in parentheses are ESD's referred to the least significant digit(s). Preferred orientation parameter G refined to 0.014(5). R_I, R_{WP}, R_e, S_P^2, and S_I^2 are defined in Ref. 13.

Atom	Site	x	y	z	B (Å^2)
Tl[a]	4(e)	0.5	0.5	0.2129(1)	0.8(1)
Ba	4(e)	0.0	0.0	0.1210(1)	0.6(1)
Ca[b]	2(a)	0.0	0.0	0.0	0.0(2)
Cu	4(e)	0.5	0.5	0.0536(1)	0.1(1)
O(1)	8(g)	0	0.5	0.0526(1)	0.4(1)
O(2)	4(e)	0.5	0.5	0.1455(1)	0.8(1)
O(3)[c]	16(n)	0.603(2)	0.5	0.2803(2)	0.5(3)

293 K	
a (Å)	3.8559(1)
c (Å)	29.4199(10)
R_I	0.041
R_{WP}	0.090
R_e	0.060
S_P^2	2.23
S_I^2	12.08

[a]Tl occupancy refined to 1.91(2) per formula unit.
[b]Ca occupancy refined to 1.09(2) per formula unit.
[c]O(3) occupancy refined to 2.00(3) per formula unit. When constrained to ideal site at $(\frac{1}{2},\frac{1}{2},z)$, B_{11} and B_{33} refined to 7.8(3) and 0.6(3) Å^2, respectively.

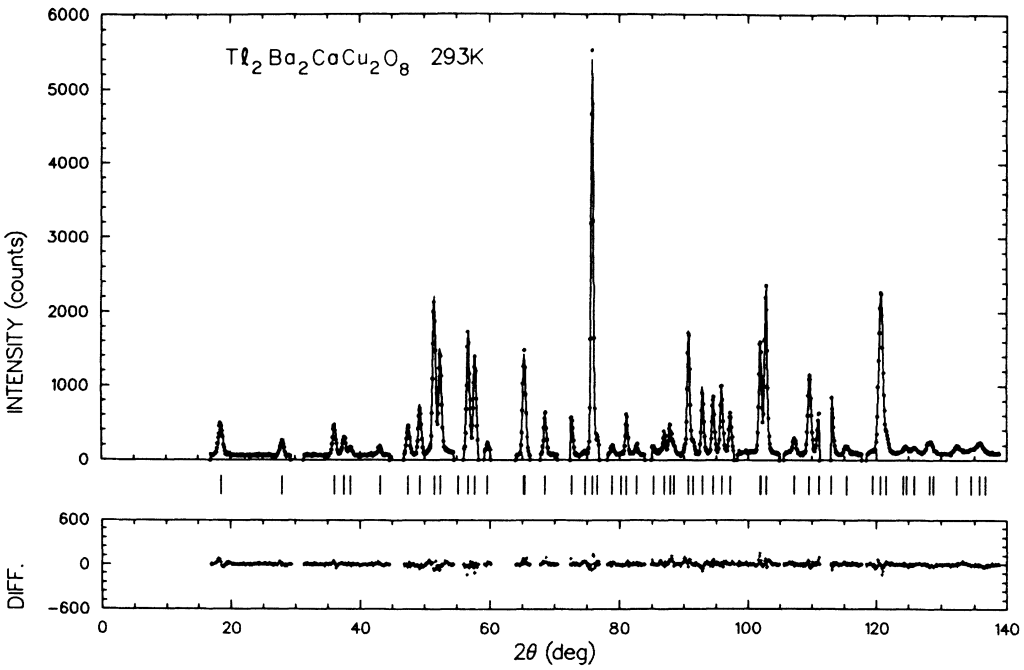

FIG. 1. Profile fit and difference plot for $Tl_2Ba_2CaCu_2O_8$ at 293 K. Short vertical markers represent allowed reflections. Peaks from impurity phase and Al sample holder have been excluded.

TABLE III. Results of Rietveld refinement for $Tl_2Ba_2Ca_2Cu_3O_{10}$ at 150 and 13 K. Scattering amplitudes for Tl, Ba, Ca, Cu, and O taken as 0.879, 0.525, 0.490, 0.7718, and 0.5805×10^{-12} cm, respectively (Ref. 16). Numbers in parentheses are ESD's referred to least significant digit(s). Preferred orientation parameter G refined to 0.085(6) and 0.076(6) at 150 and 13 K, respectively. R_I, R_{WP}, R_e, S_β^2, and S_f^2 are defined in Ref. 13.

		150 K				13 K			
Atom	Site	x	y	z	B (Å^2)	x	y	z	B (Å^2)
Tl[a]	4(*e*)	0.5	0.5	0.2195(1)	0.8(2)	0.5	0.5	0.2197(1)	0.8(2)
Ba	4(*e*)	0.0	0.0	0.1444(2)	0.5(2)	0.0	0.0	0.1445(2)	0.7(2)
Ca	4(*e*)	0.0	0.0	0.0454(2)	0.1(2)	0.0	0.0	0.0454(2)	0.1(2)
Cu(1)	2(*b*)	0.5	0.5	0.0	0.3(2)	0.5	0.5	0.0	0.2(2)
Cu(2)	4(*e*)	0.5	0.5	0.0886(1)	0.1(1)	0.5	0.5	0.0884(1)	0.1(1)
O(1)	4(*c*)	0.5	0.0	0.0	0.6(2)	0.5	0.0	0.0	0.4(2)
O(2)	8(*g*)	0.5	0.0	0.0878(1)	0.8(1)	0.5	0.0	0.0881(1)	0.9(1)
O(3)	4(*e*)	0.5	0.5	0.1650(2)	0.9(2)	0.5	0.5	0.1650(2)	1.0(2)
O(4)[b]	16(*n*)	0.601(4)	0.5	0.2750(2)	−0.5(5)	0.592(5)	0.5	0.2756(3)	0.2(6)

	150 K	13 K
a (Å)	3.8487(1)	3.8473(1)
c (Å)	35.6620(15)	35.6301(16)
R_I	0.048	0.047
R_{WP}	0.102	0.100
R_e	0.061	0.060
S_β^2	2.77	2.79
S_f^2	14.40	12.19

[a]Tl occupancy refined to 1.89(3) per formula unit at both temperatures.

[b]O(4) occupancy refined to 1.86(4) and 1.85(4) per formula unit at 150 and 13 K, respectively. When constrained to ideal site $(\frac{1}{2},\frac{1}{2},z)$, B_{11} and B_{33} refined to 6.8(5) and −0.7(5) Å^2 at 150 K, and 5.9(5) and 0.2(6) Å^2 at 13 K.

value. However, the refined occupancies for Tl and Ca (low and high, respectively) show the same trend as the x-ray values and would also be consistent with a partially substituted formulation $(Tl_{1.8}Ca_{0.2})Ba_2(Ca_{0.9}Tl_{0.1})Cu_2O_8$. However, the possibility of 5% vacancies in the Tl sites cannot be precluded. No significant oxygen occupancy was found in the site at $(\frac{1}{2},\frac{1}{2},0)$ between the Cu atoms.

The atomic positions in Table II are in excellent agreement with those determined in the x-ray study, and yield virtually identical static displacements of the O(3) atoms of about 0.4 Å from the ideal $(\frac{1}{2},\frac{1}{2},z)$ positions.

$Tl_2Ba_2Ca_2Cu_3O_{10}$

Refinement of the 150 and 13 K data sets was carried out along similar lines, including a correction for preferred orientation. The total number of reflections was 64 in each case, and the presence of static displacements was once again indicated by large and highly anisotropic apparent B's at both temperatures for the oxygens in the Tl sheets, O(4) in this case. As in the previous x-ray study, these oxygen atoms were assumed to be statistically distributed in 16(n) sites at $(x,\frac{1}{2},z)$. The results are given in Table III, and the profile fits and difference plots are illus-

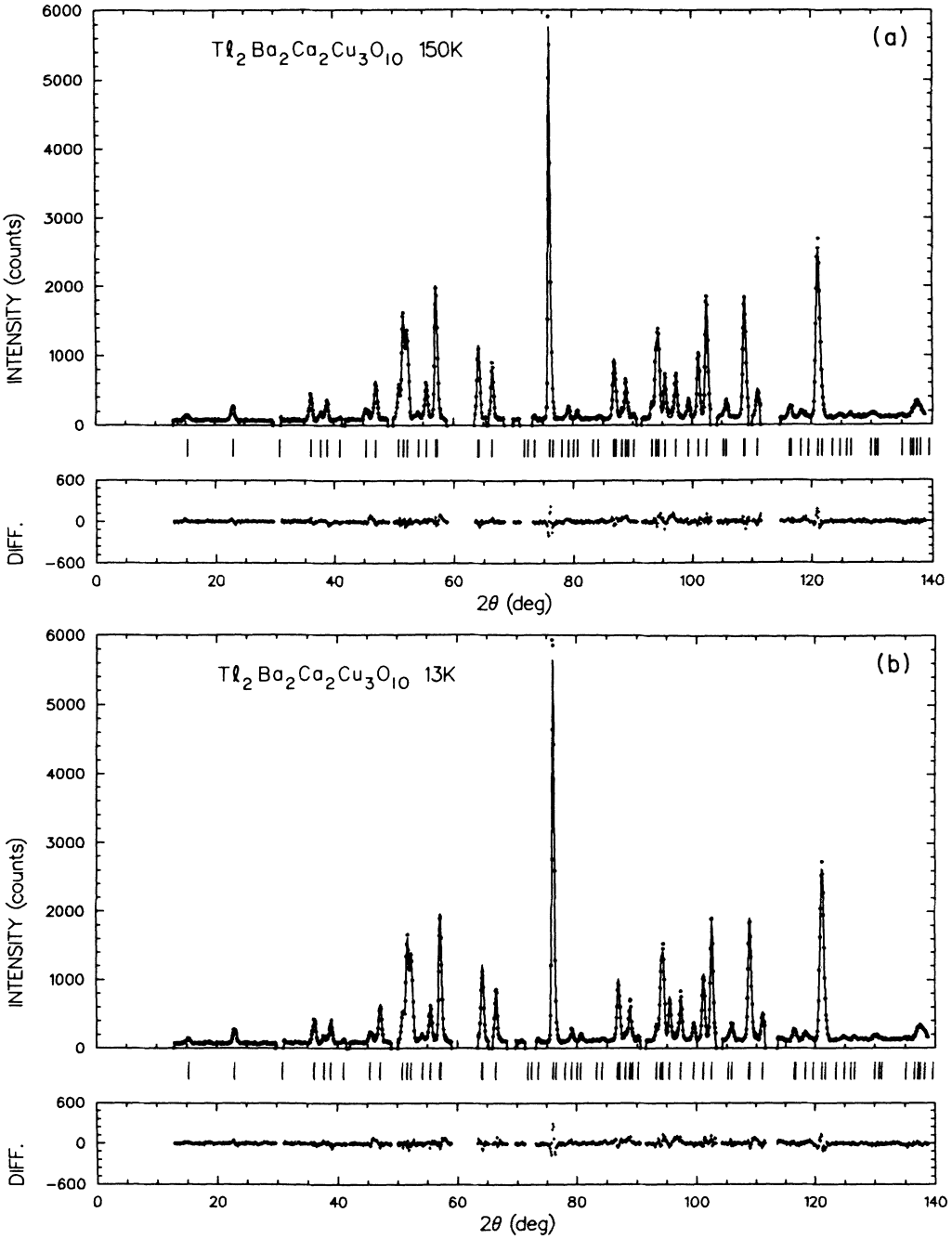

FIG. 2. Profile fit and difference plot for $Tl_2Ba_2Ca_2Cu_3O_{10}$ at 150 K (top) and 13 K (bottom).

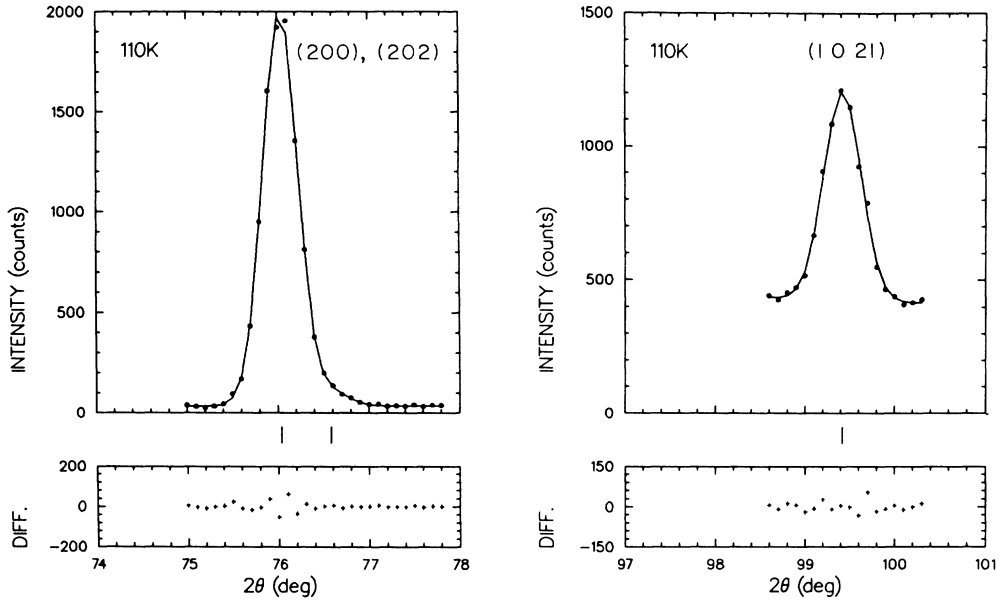

FIG. 3. Individual peak fits and difference plots for $Tl_2Ba_2Ca_2Cu_3O_{10}$ at 110 K. (200),(202) pair (left) and (1021) (right).

trated in Fig. 2. Comparison of the two sets of structural parameters reveals no significant changes of any kind above and below the superconducting transition temperature.

The refined values of the site occupancies once again indicate a possible substitution of Ca on the Tl sites, but not vice versa in this case, and also a small deficiency in the oxygen content, corresponding to the approximate composition $(Tl_{1.76}Ca_{0.25})Ba_2Ca_2Cu_3O_{9.86}$. No significant oxygen occupancy was found in the sites at $(\frac{1}{2},\frac{1}{2},0.044)$ and $(\frac{1}{2},\frac{1}{2},-0.044)$ between the Cu atoms.

The lattice parameters were determined as a function of temperature between 150 and 13 K from the peak positions of the (200) and (1021) reflections obtained from least-squares fits at several temperatures. In the former case, the fit actually involves two peaks, since (200) is overlapped by the much weaker (202) reflection, but the precision is, nevertheless, very good, as reflected by ESD's of about 0.003°. The corresponding ESD's for (1021) are about 0.006° on average. Typical fits are shown in Fig. 3.

The unit-cell parameters and cell volume are plotted as a function of temperature in Fig. 4. There are no obvious discontinuities in the transition region within experimental errors, and the only noteworthy feature is the highly anisotropic nature of the thermal expansion coefficients, with $\Delta a/a$ and $\Delta c/c$, 2.1 and 7.0×10^{-6}/K, respectively. Similar anisotropic behavior has been observed for $YBa_2Cu_3O_7$.[14,15] There is no indication in the profile fit of any distortion from tetragonal symmetry since the refined values of the half-width parameters, which would be affected by any broadening of the peaks, are essentially identical at both temperatures. If we consider only the two simple kinds of orthorhombic distortion $a_0\neq b_0\sim a_T$ ($YBa_2Cu_3O_7$ type) and $a_0\neq b_0\sim a_T\sqrt{2}$ (La_2CuO_4 type), we can estimate an upper limit on the splitting, Δa_0, from the change in half-widths (full width at half maximum) of the (200) and (220) peaks between 150 and 13 K. Least-squares fits to the (200),(202) and (220),(222) pairs yield differences of 0.000(5) and 0.016(17), respectively. In each case, $\Delta a_0/a_0$ is estimated to be less than 10^{-3}.

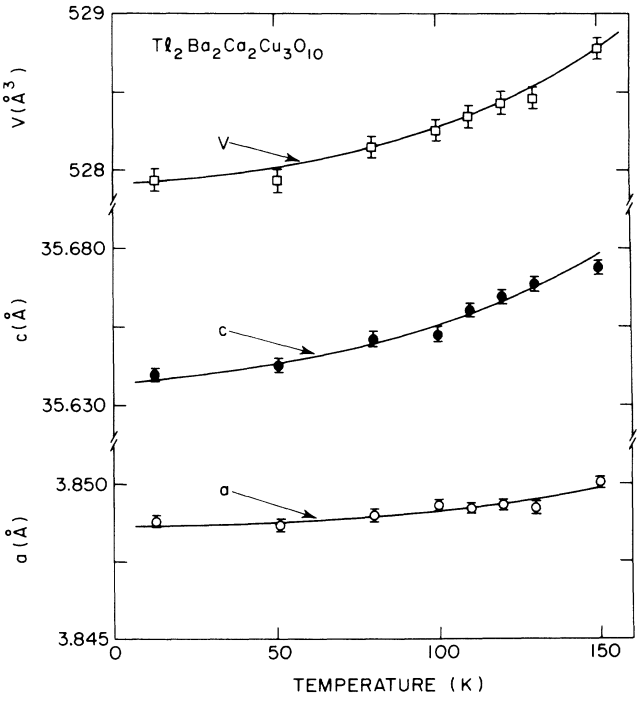

FIG. 4. Temperature dependence of unit-cell dimensions, a and c, and cell volume V, for $Tl_2Ba_2Ca_2Cu_3O_{10}$.

DISCUSSION

The structure refinement results given in Tables II and III are generally in excellent agreement with those determined in the previous x-ray studies. In particular, they provide strong support for a statistical distribution of the oxygens in the Tl planes in both compounds in sites displaced about 0.4 Å from the ideal positions in the *ab* plane (Fig. 5). The consequence of this is that on average each Tl has two short and two long Tl-O distances of about 2.5 and 3.0 Å, respectively. In each case, the planes containing these oxygens are displaced about 0.2 Å from those containing Tl.

The structural features of these compounds have been previously described[8-10] in detail and will not be discussed here except for a significant discrepancy between the neutron and x-ray values for the z coordinate of O(3) in $Tl_2Ba_2Ca_2Cu_3O_{10}$ which corresponds to a shift of about 0.2 Å along the c axis towards the neighboring Tl atom and away from the Cu(2) atom. This leads to a coordination around Tl and Cu(2), more closely resembling that in $Tl_2Ba_2CaCu_2O_8$ as can be seen from the interatomic distances listed in Table IV.

The ideal formula $Tl_2^{III}Ba_2^{II}Ca_{n-1}^{II}Cu_n^{II}O_{2n+4}$ would have all copper in the divalent state. [The valence or oxidation state of oxygen is two (O^{II}) by definition since there are no discrete oxygen-oxygen bonded units. This is true despite the fact that the real charge on oxygen is closer to one than to two.] All previously known superconductors based on copper oxide contain both Cu^{II} and Cu^{III}. There are at least four mechanisms by which Cu^{III} may be present in the phases described in this paper. First, there could be excess oxygen as proposed, but not proven, for the analogous $Bi_2Sr_2Ca_{n-1}Cu_nO_{2n+4}$ phases. Although this would produce Cu^{III}, $Tl_2Ba_2CaCu_{2-2x}^{II}Cu_{2x}^{III}O_{8+x}$, we find no evidence for such excess oxygen. In particular, there is no significant amount of oxygen between copper atoms of adjacent Cu-O layers. In any event, placing oxygen in such a position results in unreasonable interatomic distances. Secondly, there could be a cation deficiency, e.g., $Tl_{2-x}Ba_2CaCu_{2-3x}^{II}Cu_{3x}^{III}O_8$. In fact, our results are consistent with such a mechanism for producing some Cu^{III}. Thirdly, there can be substitution of Ca for Tl, i.e., $Tl_{2-x}Ca_xBa_2CaCu_{2-x}^{II}Cu_x^{III}O_8$. Again, our results are consistent with this mechanism for producing Cu^{III}. Finally, there could be some oxidation of Cu^{II} by Tl^{III}. Whether one should represent the reduced Tl species as Tl^{I} or Tl^{II} depends largely on whether or not the 6*s* electron produced is delocalized in the 6*s* band. If such delocalization occurs, the reduced Tl is best represented as Tl^{II}. However, a reduced localized Tl^{I} species could be produced. Furthermore, it is possible that the disordered oxygen of the Tl-O layer is related to a mixture of Tl^{I} and Tl^{III} within that layer.

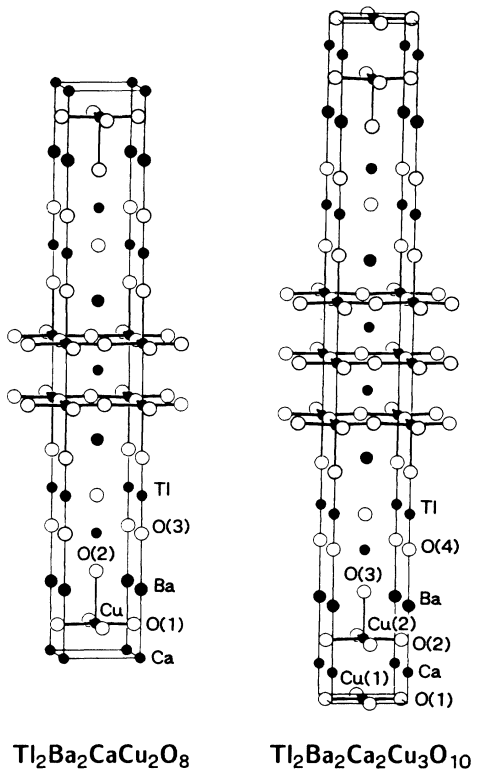

FIG. 5. Unit cells of $Tl_2Ba_2CaCu_2O_8$ and $Tl_2Ba_2Ca_2Cu_3O_{10}$.

There are then at least four mechanisms by which Cu^{III} could be produced in the idealized formulas $Tl_2Ba_2CaCu_2O_8$ and $Tl_2Ba_2Ca_2Cu_3O_{10}$. Almost certainly, at least one of these is in operation in the phases described in this paper. The degree to which each is a factor depends on the exact stoichiometry which cannot be precisely con-

TABLE IV. Cu-O and Tl-O distances in Å in $Tl_2Ba_2CaCu_2O_8$ and $Tl_2Ba_2Ca_2Cu_3O_{10}$ from the neutron structure refinement. Post factors represent the number of such bonds to each Cu or Tl atom.

$Tl_2Ba_2CaCu_2O_8$ (293 K)			$Tl_2Ba_2Ca_2Cu_3O_{10}$ (150 K)		
Cu-O(1)	1.928	(×4)	Cu(1)-O(1)	1.924	(×4)
Cu-O(2)	2.704(4)	(×1)	Cu(2)-O(2)	1.925	(×4)
			Cu(2)-O(3)	2.725(8)	(×1)
Tl-O(2)	1.983(4)	(×1)	Tl-O(3)	1.944(8)	(×1)
Tl-O(3)	2.022(7)	(×1)	Tl-O(4)	2.017(8)	(×1)
Tl-O(3)	2.470(5)	(×2)	Tl-O(4)	2.470(10)	(×2)
Tl-O(3)	3.027(6)	(×2)	Tl-O(4)	3.015(12)	(×2)

trolled at this time. It is likely that the variations in T_c for these phases with apparent fixed n is due to variations in stoichiometry with resulting variations in Cu^{III} content. On the other hand, the variations in T_c may also be attributed to intergrowth regions where n differs from that of the predominant phase. For the $n=1$ phase, $Tl_2Ba_2CuO_6$, current evidence suggests that the only plausible mechanism for producing Cu^{III} is the oxidation of Cu^{II} by Tl^{III}.

This work was supported in part by the U.S. Department of Energy, Division of Materials Sciences, under Contract No. DE-AC02-76CH00016.

[1]Z. Z. Sheng and A. M. Hermann, Nature **332**, 55 (1988).

[2]Z. Z. Sheng, A. M. Hermann, A. El Ali, C. Almasan, J. Estrada, T. Datta, and R. J. Matson, Phys. Rev. Lett. **60**, 937 (1988).

[3]Z. Z. Sheng and A. M. Hermann, Nature **332**, 138 (1988).

[4]R. M. Hazen, L. W. Finger, R. J. Angel, C. T. Prewitt, N. L. Ross, C. G. Hadidiacos, P. J. Heaney, D. R. Veblen, Z. Z. Sheng, A. El Ali, and A. M. Hermann, Phys. Rev. Lett. **60**, 1657 (1988).

[5]M. A. Subramanian, C. C. Torardi, J. C. Calabrese, J. Gopalakrishnan, K. J. Morrissey, T. R. Askew, R. B. Flippen, U. Chowdhry, and A. W. Sleight, Science **239**, 1015 (1988).

[6]J. M. Tarascon, Y. LePage, P. Barboux, B. G. Bagley, L. H. Greene, W. R. McKinnon, G. W. Hull, M. Giroud, and D. M. Hwang, Phys. Rev. B **37**, 9382 (1988).

[7]S. A. Sunshine, T. Siegrist, L. F. Schneemeyer, D. W. Murphy, R. J. Cava, B. Batlogg, R. B. van Dover, R. M. Fleming, S. H. Glarum, S. Nakahara, R. Farrow, J. J. Krajewski, S. M. Zahurak, J. V. Waszczak, J. H. Marshall, P. Marsh, L. W. Rupp, Jr., and W. F. Peck, Phys. Rev. B **38**, 893 (1988).

[8]C. C. Torardi, M. A. Subramanian, J. C. Calabrese, J. Gopalakrishnan, K. J. Morrissey, T. R. Askew, R. B. Flippen, U. Chowdhry, and A. W. Sleight, Science **240**, 631 (1988).

[9]C. C. Torardi, M. A. Subramanian, J. C. Calabrese, J. Gopalakrishnan, E. M. McCarron, K. J. Morrissey, T. R. Askew, R. B. Flippen, U. Chowdhry, and A. W. Sleight, Phys. Rev. B **38**, 225 (1988).

[10]M. A. Subramanian, J. C. Calabrese, C. C. Torardi, J. Gopalakrishnan, T. R. Askew, R. B. Flippen, K. J. Morrissey, U. Chowdhry, and A. W. Sleight, Nature **332**, 420 (1988).

[11]H. M. Rietveld, J. Appl. Crystallogr. **2**, 65 (1969).

[12]A. W. Hewat, Atomic Energy Research Establishment, Harwell, Report No. R7350, 1973 (unpublished).

[13]H. G. Scott, J. Appl. Crystallogr. **16**, 159 (1983).

[14]P. M. Horn, D. T. Keane, G. A. Held, J. L. Jordan-Sweet, D. L. Kaiser, F. Holtzberg, and T. M. Rice, Phys. Rev. Lett. **59**, 2772 (1987).

[15]H. You, J. D. Axe, X. B. Kan, S. Hashimoto, C. S. Moss, J. Z. Liu, G. W. Crabtree, and D. J. Lam (unpublished).

[16]L. Koester and Y. B. Yelon, *Neutron Cross Section Data* (Netherlands Energy Research Foundation, ECN, Petten, 1983).